
Adaptive Nonparametric Variational Autoencoder

Tingting Zhao¹, Zifeng Wang¹, Aria Masoomi¹, and Jennifer G. Dy¹

¹Electrical and Computer Engineering Department, Northeastern University
 $\{tzhao,zifengwang,amasoomi,jdy\}@ece.neu.edu$

Abstract

Clustering is used to find structure in unlabeled data by grouping similar objects together. Cluster analysis depends on the definition of similarity in the feature space. In this paper, we propose an Adaptive Nonparametric Variational Autoencoder (AdapVAE) to perform end-to-end feature learning from raw data jointly with cluster membership learning through a Nonparametric Bayesian modeling framework with deep neural networks. It has the advantage of avoiding pre-definition of similarity or feature engineering. Our model relaxes the constraint of fixing the number of clusters in advance by assigning a Dirichlet Process prior on the latent representation in a low-dimensional feature space. It can adaptively detect novel clusters when new data arrives based on a learned model from historical data in an online unsupervised learning setting. We develop a joint online variational inference algorithm to learn feature representations and cluster assignments via iteratively optimizing the evidence lower bound (ELBO). Our experimental results demonstrate the capacity of our modelling framework to learn the number of clusters automatically using data, the flexibility to detect novel clusters with emerging data adaptively, the ability of high quality reconstruction and generation of samples without supervised information and the improvement over state-of-the-art end-to-end clustering methods in terms of accuracy on both image and text corpora benchmark datasets.

1 Introduction

Clustering is an important unsupervised learning problem in machine learning. It is the task of grouping similar objects together such that there is high intra-cluster similarity and low inter-cluster similarity among different objects. Cluster analysis depends on the definition of similarity or distance among objects. Similarity or distance, in turn, depends on the feature space, in which the representation of the data is defined. For example, traditional K-means clustering algorithm (MacQueen et al., 1967) takes advantage of the Euclidian distance among points in a feature space. Thus, to apply such algorithms, the user needs to determine the choice of the feature space to represent the raw data. Our paper provides an end-to-end learning from raw data while conducting clustering jointly. We learn the feature space through deep neural networks without having to pre-define similarity or feature engineering. Moreover, we would like to have our unsupervised learning algorithm to continually learn and discover novel clusters as it encounters data in an online setting.

Recent research work (Dilokthanakul et al., 2016; Jiang et al., 2017; Kilinc and Uysal, 2018) has focused on combining deep generative models to learn good representations of the original data and probabilistic models to conduct clustering analysis. Johnson et al. (2016) have proposed a general modeling and inference framework that combines the complementary strengths of probabilistic graphical models and deep learning methods. Deep Embedded Clustering (DEC) (Xie et al., 2016) has focused on simultaneously learning feature representations and cluster assignments using deep neural networks. DEC has achieved good performance in clustering but it can not model the generative process of the data. To resolve this issue, Variational Deep Embedding (VaDE) (Jiang et al., 2017)

has been proposed to combine Variational Autoencoder (VAE) (Kingma and Welling, 2014) and a Gaussian Mixture Model (GMM) to learn representations of the data while capable of performing clustering and generating samples.

However, there still exist several limitations of the latest existing methods: (1) the number of clusters needs to be fixed in advance; (2) they can not detect potential novelty when new data arrives based on a learned model from historical data or they are just able to classify all the emerging novelty as an *outlier* class instead of further categorizing them into different clusters according to the characteristics of the data (Williams et al., 2002; Kodirov et al., 2015; Amarbayasgalan et al., 2018; Masana et al., 2018) (3) the prior on the latent representation is restricted to a GMM with a fixed finite number of mixture components.

To resolve all these limitations, we develop an Adaptive Nonparametric Variational Autoencoder (AdapVAE) modelling framework, which uses VAE to learn deep latent representation of the data while performing clustering via Dirichlet Process Mixture Model (DPMM). The diagram of AdapVAE providing an overview of our work is shown in Figure 1. It learns the cluster membership of the data through a Dirichlet Process (DP) prior, which allows the model to grow with the data. To detect emerging clusters as the new data arrives, our model jointly trains the proposed AdapVAE on the new data in an online fashion based on estimates from historical data. Moreover, high quality generated samples can be obtained using AdapVAE. This process is shown in Figure 1b.

However, inference for AdapVAE is challenging. We have developed an online variational inference algorithm to maximize an objective function which jointly takes into account the reconstruction error of the VAE and the DPMM fit on the latent representation. It alternately refines cluster assignments and improves latent feature representation in an iterative way. Our online variational algorithm combines advances from the Stochastic Gradient Variational Bayes (SGVB) estimator and the reparameterization trick in VAE (Kingma and Welling, 2014) and the advantages of memoized online variational inference strategies for DPMM (Hughes and Sudderth, 2013).

Our experimental results demonstrate that our modelling framework is able to detect novel clusters that emerge as new data arrives in an online setting. We use MNIST (LeCun et al., 1998) to show that our model is able to generate high quality samples. Our approach also achieves state-of-the-art clustering accuracy on image and text benchmark datasets including MNIST, STL (Coates et al., 2011) and REUTERS (Lewis et al., 2004). We also perform a comprehensive comparison with several state-of-the-art methods such as VaDE (Jiang et al., 2017), DEC (Xie et al., 2016) using multiple clustering quality evaluation metrics. Unlike previous methods, our approach does not need K-means or GMM as clustering initialization. Our model starts with one cluster and adaptively learns the number of clusters and cluster assignments using DPMM on the latent representation space.

To summarize, we introduce a novel adaptive nonparametric variational autoencoder clustering algorithm, AdapVAE, that can (1) learn the structure of feature space while clustering through deep representation; (2) automatically learn the number of clusters and detect novel clusters adaptively when new data arrives. Our experimental results show that AdapVAE achieves state-of-the-art clustering results on both image and text benchmark datasets.

2 Adaptive Nonparametric Variational Autoencoder

Problem Statement

Let \mathbf{x}_n denote the n th observation, for $n = 1, 2, \dots, N$, where N denotes the total number of observations. Given unlabeled data $\mathbf{x}_n \in X$, where X represents the data space, it is our interest to learn a low-dimensional latent representation for \mathbf{x}_n while simultaneously clustering the set of N observations in the latent space. For example, \mathbf{x}_n can represent an image of millions of pixels and we target to group similar images together in a low-dimensional latent space. Unlike existing methods (Dilokthanakul et al., 2016; Xie et al., 2016; Jiang et al., 2017) that fix the number of clusters in advance, we learn the number of clusters dynamically according to the complexities of the data. Our model also aims to learn novel clusters adaptively with new emerging data based on a learned model from historical data in an unsupervised online learning setting. Our AdapVAE modelling framework is built based on a combination of DPMM and VAE.

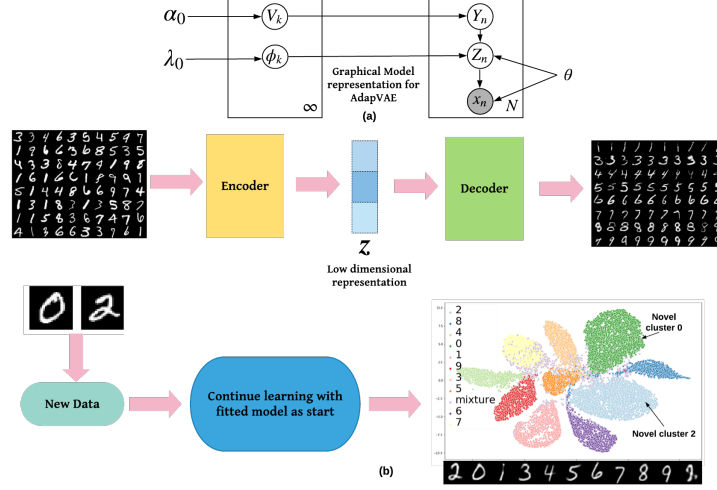


Figure 1: An overview of the work flow for our modelling framework together with the graphical model representation for AdapVAE, where the latent representation learnt in VAE are treated as observations when training DPMM. The figure is best viewed in color.

2.1 Dirichlet Process Mixture Models

The Dirichlet process (DP) is a random probability measure that can be used as a non-parametric prior. It can be seen as a countably infinite sum of atomic measures, where each partition is assigned with an independent parameter from a common distribution. A constructive definition of DP via a stick-breaking process was provided by Sethuraman and Tiwari (1982), which is reviewed below.

A DP is characterized by a base distribution G_0 and a parameter α and is denoted as $\text{DP}(G_0, \alpha)$. A stick-breaking prior is of the form $G(\cdot) = \sum_{k=1}^{\infty} \pi_k \delta_{\theta_k}$, where δ_{θ_k} is a discrete measure concentrated at $\theta_k \sim G_0$, which is a random sample from the base distribution G_0 (Ishwaran and James, 2001) and can be seen as the parameters of the component distribution of a mixture of distributions with mixing proportion π_k . The π_k s are random weights independent of G_0 but satisfy $0 \leq \pi_k \leq 1$ and $\sum_{k=1}^{\infty} \pi_k = 1$. The weights π_k can be drawn through an iterative process:

$$\pi_k = \begin{cases} v_1, & \text{if } k = 1, \\ v_k \prod_{j=1}^{k-1} (1 - v_j), & \text{for } k > 1, \end{cases}$$

where $v_k \sim \text{Beta}(1, \alpha)$ so that we obtain the stick-breaking construction of $\text{DP}(G_0, \alpha)$. Assume that z comes from a mixture of Gaussian distribution and the number of mixture components is unknown. DPMM is often adopted to sidestep the issue of determining the number of mixture components for clustering tasks (Blei et al., 2006; Ahmed and Xing, 2008).

2.2 Variational Autoencoder

In order to learn the low-dimensional representation of the data space X while maintaining high quality reconstruction, VAE (Kingma and Welling, 2014) is a natural choice. In an autoencoder, the encoder transforms the data via a mapping $f_{\psi} : X \rightarrow Z$, where Z represents the (low-dimensional) latent feature space and f_{ψ} is often chosen as a deep neural network due to its powerful function approximation capability (Hornik, 1991) and good feature learning capabilities (Kingma et al., 2014; Nalisnick et al., 2016), where ψ represents the parameters to be learned in the neural network. Similarly, $g_{\theta} : Z \rightarrow X$ represents the decoder neural network, which maps the latent representation to reconstruct the original data.

In a VAE, instead of serving as the output from a deterministic function f_{ψ} , a latent representation z is sampled from $q_{\psi}(z|x)$ and is passed to the decoder $p_{\theta}(x|z)$ to reconstruct the original input x as \hat{x} , where it is assumed that $q_{\psi}(z|x) = \mathcal{N}(\mu, \sigma^2)$ and $f_{\psi}(x) = (\mu, \log \sigma^2 I)$, where $f_{\psi}(x)$ is a neural network and $(\mu, \log \sigma^2 I)$ represents the output of the neural network. The parameters

θ and ψ are learned by minimizing the reconstruction error, which is equivalent to maximizing $\mathbb{E}_{z \sim q_\psi(z|x)} (\log p_\theta(x|z))$. VAE has good feature learning capacities but it is not able to perform clustering tasks.

2.3 AdapVAE and Its Generative Process

Our proposed AdapVAE extends traditional VAE by replacing the standard Gaussian distribution on the latent representation z with a DP Gaussian mixture model on z , which allows it to perform clustering tasks. It is able to grow the number of clusters on the latent space adaptively and learn better latent representations simultaneously. It can also learn novel clusters if new data arrives by updating the posterior AdapVAE with new data starting from a learned model based on historical data. We first introduce the generative process of AdapVAE. The graphical model is provided in Figure 1a.

Assume that the latent representation of the observation is a realization from DP Gaussian Mixture,

$$G \sim \text{DP}(\alpha_0, G_0), \quad G_0 = \text{NW}(\boldsymbol{\lambda}_0), \quad G \stackrel{\Delta}{=} \sum_{i=1}^{\infty} w_k \delta_{\phi_k}, \quad \phi_k = (\boldsymbol{\mu}_k^*, \boldsymbol{\sigma}_k^*) \sim \text{NW}(\boldsymbol{\lambda}_0),$$

and NW represents the Normal-Wishart distribution with parameters $\boldsymbol{\lambda}_0$, which we assume as the base distribution G_0 of DP.

The data can be described as generated from the following process:

- Draw $V_i|\alpha_0 \sim \text{Beta}(1, \alpha_0)$, $i = \{1, 2, \dots\}$.
- Draw $(\boldsymbol{\mu}_k^*, \boldsymbol{\sigma}_k^*)|G_0 \sim G_0$, $i = \{1, 2, \dots\}$.
- For the n th data point \mathbf{x}_n :
 - (a) Draw a cluster membership $Y_n \sim \text{Cat}(\pi(\mathbf{v}))$, where

$$\pi_k = \begin{cases} v_1, & \text{if } k = 1, \\ v_k \prod_{j=1}^{k-1} (1 - v_j), & \text{for } k > 1. \end{cases}$$

- (b) Draw a latent representation vector $Z_n|Y_n = k \sim \mathcal{N}(\boldsymbol{\mu}_k^*, \boldsymbol{\sigma}_k^{*2})$.
- (c) Generate the n th observation \mathbf{x}_n from $X_n|Z_n = z_n \sim \mathcal{N}(\boldsymbol{\mu}(z_n; \theta), \boldsymbol{\sigma}^2(z_n, \theta))$, where $(\boldsymbol{\mu}(z_n; \theta), \boldsymbol{\sigma}^2(z_n, \theta)) = g_\theta(z_n; \tau)$ is a neural network, which represents the decoder to reconstruct the observation \mathbf{x}_n from the latent vector z_n .

The joint probability density for the generative process is

$$\begin{aligned} p(\mathbf{x}, \mathbf{y}, \mathbf{z}, \boldsymbol{\phi}, \mathbf{v}) &= p(\mathbf{x}|\mathbf{z}; \tau)p(\mathbf{z}|\mathbf{y})p(\mathbf{y}|\mathbf{v})p(\mathbf{v})G_0(\boldsymbol{\phi}|\boldsymbol{\lambda}_0) \\ &= \prod_{n=1}^N \mathcal{N}(\mathbf{x}_n|\boldsymbol{\mu}(z_n; \theta), \boldsymbol{\sigma}^2(z_n, \theta)\mathbf{I}) \prod_{k=1}^{\infty} \mathcal{N}(z_n|\boldsymbol{\mu}_k^*, \boldsymbol{\sigma}_k^2\mathbf{I})P(Y_n = k|\pi(\mathbf{v})) \\ &\quad \text{Beta}(v_k|1, \alpha_0)G_0(\boldsymbol{\phi}_k|\boldsymbol{\lambda}_0). \end{aligned}$$

3 Variational Inference for AdapVAE

Since the posterior distribution under DPMMs is intractable, approximate inference methods are required. Variational inference provides an approximation for the posterior p by casting inference as an optimization problem. It aims to find a surrogate distribution q that is the most similar to the distribution p of interest over a class of tractable distributions. Given the generative process in Section 2.3, the marginal log-likelihood for data \mathbf{x} is

$$\log p(\mathbf{x}) = \log \int_{\mathbf{z}} \sum_{\mathbf{y}} \int_{\mathbf{v}} \int_{\boldsymbol{\phi}} p(\mathbf{x}, \mathbf{y}, \mathbf{z}, \boldsymbol{\phi}, \mathbf{v}) dz d\mathbf{v} d\boldsymbol{\phi},$$

Using Jensen's inequality, we can obtain that

$$\log p(\mathbf{x}) \geq \mathbb{E}_{q(\mathbf{y}, \mathbf{z}, \boldsymbol{\phi}, \mathbf{v}|\mathbf{x})} \left\{ \log \frac{p(\mathbf{x}, \mathbf{y}, \mathbf{z}, \boldsymbol{\phi}, \mathbf{v})}{q(\mathbf{y}, \mathbf{z}, \boldsymbol{\phi}, \mathbf{v}|\mathbf{x})} \right\} = \mathcal{L}_{\text{ELBO}}(\mathbf{x}), \quad (1)$$

where $q(\mathbf{y}, \mathbf{z}, \boldsymbol{\phi}, \mathbf{v}|\mathbf{x})$ is the variational posterior distribution used to approximate the true posterior $p(\mathbf{y}, \mathbf{z}, \boldsymbol{\phi}, \mathbf{v}|\mathbf{x})$ and $\mathcal{L}_{\text{ELBO}}$ is the Evidence Lower Bound (ELBO). Minimizing the Kullback-Leibler (KL) divergence between $q(\mathbf{y}, \mathbf{z}, \boldsymbol{\phi}, \mathbf{v}|\mathbf{x})$ and $p(\mathbf{y}, \mathbf{z}, \boldsymbol{\phi}, \mathbf{v}|\mathbf{x})$ is equivalent to maximizing the ELBO. We assume $q(\mathbf{y}, \mathbf{z}, \boldsymbol{\phi}, \mathbf{v}|\mathbf{x})$ can be factorized as $q_\psi(\mathbf{z}|\mathbf{x})q(\mathbf{y})q(\mathbf{v})q(\boldsymbol{\phi})$. Thus, the ELBO is

$$\begin{aligned}
& \mathbb{E}_{q(\mathbf{y}, \mathbf{z}, \boldsymbol{\phi}, \mathbf{v} | \mathbf{x})} \left[\log \frac{p(\mathbf{x} | \mathbf{z}) p(\mathbf{z} | \mathbf{y}, \boldsymbol{\phi}) p(\mathbf{y} | \mathbf{v}) p(\mathbf{v}) p(\boldsymbol{\phi})}{q_{\psi}(\mathbf{z} | \mathbf{x}) q(\mathbf{y} | \mathbf{x}) q(\mathbf{v}) q(\boldsymbol{\phi} | \mathbf{x})} \right] \\
&= \mathbb{E}_{q(\mathbf{y}, \mathbf{z}, \boldsymbol{\phi}, \mathbf{v} | \mathbf{x})} [\log p(\mathbf{x} | \mathbf{z})] + \mathbb{E}_{q(\mathbf{y}, \mathbf{z}, \boldsymbol{\phi}, \mathbf{v} | \mathbf{x})} [\log p(\mathbf{z} | \mathbf{y}, \boldsymbol{\phi})] \\
&\quad - \mathbb{E}_{q(\mathbf{y}, \mathbf{z}, \boldsymbol{\phi}, \mathbf{v} | \mathbf{x})} [\log q_{\psi}(\mathbf{z} | \mathbf{x})] \\
&\quad + \mathbb{E}_{q(\mathbf{y}, \mathbf{z}, \boldsymbol{\phi}, \mathbf{v} | \mathbf{x})} [\log p(\mathbf{y} | \mathbf{v})] + \mathbb{E}_{q(\mathbf{y}, \mathbf{z}, \boldsymbol{\phi}, \mathbf{v} | \mathbf{x})} [\log p(\mathbf{v})] \\
&\quad - \mathbb{E}_{q(\mathbf{y}, \mathbf{z}, \boldsymbol{\phi}, \mathbf{v} | \mathbf{x})} [\log q(\mathbf{y} | \mathbf{x})] - \mathbb{E}_{q(\mathbf{y}, \mathbf{z}, \boldsymbol{\phi}, \mathbf{v} | \mathbf{x})} [\log q(\mathbf{v})] \\
&\quad - \mathbb{E}_{q(\mathbf{y}, \mathbf{z}, \boldsymbol{\phi}, \mathbf{v} | \mathbf{x})} [\log q(\boldsymbol{\phi} | \mathbf{x})] + \mathbb{E}_{q(\mathbf{y}, \mathbf{z}, \boldsymbol{\phi}, \mathbf{v} | \mathbf{x})} [\log p(\boldsymbol{\phi})]
\end{aligned} \tag{2}$$

In Equation 2, only the first three terms contribute to optimizing the neural network parameters θ , ψ and latent representation \mathbf{z} . We denote this part in the ELBO as $\mathcal{L}_{\text{ELBO-VAE}}$, which is derived by combining the first three terms involving \mathbf{z} in Equation 2. Derivation details can be found in Section 1 in the Supplement.

$$\begin{aligned}
\mathcal{L}_{\text{ELBO-VAE}}(\mathbf{x}) = & -\frac{1}{2L} \sum_{l=1}^L \sum_{k=1}^T N_k \nu_k \left\{ \text{Tr}(S_k W_k) + (\bar{\mathbf{z}}_k - \mathbf{m}_k)^T W_k (\bar{\mathbf{z}}_k - \mathbf{m}_k) \right\} \\
& - \frac{1}{2} \frac{1}{L} \sum_{i=1}^N \sum_{j=1}^D \left(\log(\sigma_x^2)_j^{(l)} + \left(\mathbf{x}_{ij} - (\boldsymbol{\mu}_x)_j^{(l)} \right)^2 / (\sigma_x^2)_j^{(l)} \right) + \frac{1}{2} \log(\text{Det}(2\pi e \Sigma)).
\end{aligned} \tag{3}$$

We adopt alternating optimization strategy to maximize the ELBO. We update the VAE parameters (θ and ψ) and the latent variable (\mathbf{z}) given the current estimates of the DPMM parameters. To update neural network parameters θ , ψ and latent representation \mathbf{z} , we maximize $\mathcal{L}_{\text{ELBO-VAE}}(\mathbf{x})$ using SGVB and representation trick. Note that in Equation 10, $\bar{\mathbf{z}}_k$ is a function of parameters θ and ψ , which are optimized through stochastic gradient backpropagation, where $\bar{\mathbf{z}}_k = \frac{1}{N_k} \sum_{n=1}^N \gamma_{nk} \hat{\mathbf{z}}_n$ and $\hat{\mathbf{z}}_n = \boldsymbol{\mu}(\mathbf{x}_n; \psi)$. In Equation 10, the first term comes from training DPMM on \mathbf{z} . The second term and third term stem from the output from the decoder and encoder respectively, where Σ represents the diagonal covariance matrix of the encoder. We provide a summary of notations in Table S1. When updating the DPMM parameters, the latent representation \mathbf{z} is treated as the observations for DPMM. Thus, the updates for the local cluster membership assignment parameter \mathbf{y} , global parameters $\boldsymbol{\phi}$ and \mathbf{v} simplifies to the updates in variational inference for DPMM (Blei et al., 2006).

Table 1: Notations in the ELBO.

Notations in the ELBO

N : the total number of observations.
L : the number of samples we obtain when using SGVB and representation trick for VAE.
Σ : the diagonal covariance matrix of the encoder.
\mathbf{x}_n : the n th observation.
$p(\mathbf{y}_i = k) = \gamma_{ik}$: the probability of the i th observation in the k th cluster.
$N_k = \sum_{n=1}^N \gamma_{nk}$: the sum of the probability of the total N observations in the k th cluster.
$\hat{\mathbf{z}}_n = \boldsymbol{\mu}(\mathbf{x}_n; \psi)$: the estimated mean of the latent representation from the encoder given \mathbf{x}_n .
$\bar{\mathbf{z}}_k = \frac{1}{N_k} \sum_{n=1}^N \gamma_{nk} \hat{\mathbf{z}}_n$: the weighted mean of the k th cluster in the latent representation space.
$S_k = \frac{1}{N_k} \sum_{n=1}^N \gamma_{nk} (\hat{\mathbf{z}}_n - \bar{\mathbf{z}}_k)(\hat{\mathbf{z}}_n - \bar{\mathbf{z}}_k)^T$.
$\beta_k = \beta_0 + N_k$: the scalar precision for \mathbf{z}_k in the Normal-Wishart distribution.
$\mathbf{m}_k = \frac{1}{\beta_k} (\beta_0 \mathbf{m}_0 + N_k \bar{\mathbf{z}}_k)$: the updated formula for the mean of the Normal-Wishart distribution for the k th cluster, where the prior \mathbf{m}_0 is usually chosen as a zero vector.
$W_k^{-1} = W_0^{-1} + N_k S_k + \frac{\beta_0 N_k}{\beta_0 + N_k} (\bar{\mathbf{z}}_k - \mathbf{m}_0)(\bar{\mathbf{z}}_k - \mathbf{m}_0)^T$: the updated formula for W_k^{-1} , the parameter of Normal-Wishart distribution.
$\nu_k = \nu_0 + N_k$: updated degrees of freedom of the Normal-Wishart distribution for the k th cluster.
ϕ : the variational parameters of the Normal Wishart mixing components in the DP.

In order to detect novelty in an online fashion using AdapVAE, instead of using the standard variational inference for DPMM, we follow Hughes and Sudderth (2013)'s memoized online variational inference strategy. AdapVAE visits each batch of the full dataset in turn and updates a cached set of sufficient statistics which capture the characteristics of the entire dataset. It incrementally updates the local and

global parameters of DPMM. To relax the constraint of a restrictive fixed truncation in the number of mixture components, it introduces *birth* and *merge* moves to improve the ELBO. Birth moves add new mixture components in DPMM and merge moves eliminate redundancy by merging clusters, which allow adaptive creation and pruning of clusters online. Details are summarized in Algorithm 1.

Algorithm 1 Variational Online Inference for AdapVAE

```

1: Initialization:
   Initialize variational distributions and the hyperparameters for DPMM.
2: for epoch = 1, 2, . . . do
3:   for  $i = 1, 2, \dots, M$  do
4:     Select the  $i$ th batch of the observations randomly.
5:     for  $t = 1, 2, \dots, T$  do
6:       Update the parameters of the VAE according to  $\omega^{(t+1)} = \omega^{(t)} + \eta \frac{\partial L_{\text{ELBO-VAE}}(\mathbf{x})}{\partial \omega^{(t)}}$  to maximize
          the  $L_{\text{ELBO}}(\mathbf{x})$  in Equation 10 given current DPMM parameters, where  $\omega = \{\theta, \psi\}$  denoting the
          parameters in both the encoder and decoder and  $\eta$  denotes the learning rate and the partial derivative
          is computed via stochastic gradient backpropagation.
7:     end for
8:     Compute the deep representation  $\mathbf{z}$  of the observations in the  $i$ th batch using the encoder  $\mu = f_\psi(\mathbf{x})$ .
9:     Divide the  $i$ th batch of latent representation  $\mathbf{z}$  into  $L$  batches and  $\mathbf{z}$  is treated as the observation for
          DPMM.
10:    while The ELBO of DPMM has not converged do
11:      Visit each distinct batch  $b$  of  $\mathbf{z}$  once in a full pass of the latent representation in the  $i$ th batch.
12:      Incrementally updating the local and global parameters of DPMM related to batch  $b$  according to
          Equation 10 and Equation 11 in Hughes and Sudderth (2013).
13:      Add birth moves to create new mixture cluster components.
14:      Merge two randomly selected components if the ELBO improves.
15:      Compute the ELBO of DPMM under mean field assumptions.
16:    end while
17:  end for
18: end for
19: Output: Learned AdapVAE, variational distributions, deep latent representation and cluster
          assignment for each observation.

```

4 Experiments

Our method is evaluated using both text and image benchmark datasets, which have been used in state-of-the-art methods (Jiang et al., 2017; Xie et al., 2016). A brief description of the datasets and the implementation details are provided in Section 4.1 and 4.2.

We provide qualitative and quantitative clustering quality comparison among DEC, VaDE and AdapVAE using multiple metrics. A list of the methods in comparison are shown in Table 4. All the competing methods fix the number of clusters the same as the ground truth. AdapVAE starts with one cluster and learns the number of clusters automatically. The best and average performance across multiple replications are provided in Table 4 and Table 1 in the Supplement. Finally, we use MNIST to demonstrate the clustering pattern of AdapVAE and the quality of generated samples.

4.1 Datasets

We conduct experiments on two image and one text data benchmarks. Detailed information for each dataset is described in the Supplement and we provide summary statistics in Table 2.

Table 2: Summary statistics for benchmark datasets.

Dataset Type	Dataset	# Samples	Dimension	Classes
Image	MNIST	70000	784	10
Text	REUTERS-10K	10000	2000	4
Image	STL-10	13000	2048	10

4.2 Implementation Details

To make a fair comparison with DEC and VaDE, we adopt their neural network architecture. The

pipeline is $d - 500 - 500 - 2000 - l$ and $l - 2000 - 500 - d$ for the encoder and decoder, respectively, where d and l denote the dimensionality of the input and latent feature. All layers are fully connected and a sampling layer with reparametrization trick bridges the encoder and decoder. We adopt the same pretrained Stacked Autoencoder in VaDE as the initialization for the neural network. Adam optimizer (Kingma and Ba, 2014) is used as the optimization engine to update the neural network. The batch size is set to 1500. The learning rate for Reuters-10K and STL-10 is set as 0.002 and 0.0002 for MNIST with a common decay rate of 0.9 for every epoch. For the clustering initialization, DEC and VaDE start with K-means or GMM and fix the number of clusters as the ground truth. AdapVAE starts with one cluster and learns the number of clusters automatically.

4.3 Evaluation Metrics

Standard clustering evaluation metric, unsupervised clustering accuracy (ACC) is used to compare different methods, and is defined as $ACC = \max_m \frac{\sum_{i=1}^N 1\{l_i = m(c_i)\}}{N}$, where N is the total number of observations, l_i is the ground-truth label, c_i is the cluster assignment by the algorithm and m ranges over all possible one-to-one mappings between clusters and labels.

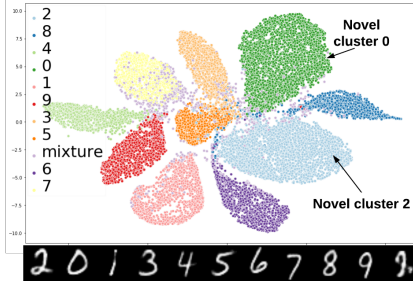
We also use other standard metrics including Normalized Mutual Information (NMI), Adjusted Random Index (ARI), Homogeneity Score (HS) and V-measure Score (VM) to compare different clustering with different number of clusters. They are all normalized metrics ranging from zero to one with value one representing perfect clustering as the ground truth. More details are provided in Section 3 in the Supplement.

4.4 Online Novelty Detection and Clustering Quality

In this section, we demonstrate AdapVAE can detect novel clusters when new data arrives in an online fashion using MNIST. MNIST includes 10 classes of hand-written digit samples ranging from zero to nine. Denote $\chi = \{1, 3, 4, 5, 6, 7, 8, 9\}$. Using MNIST, we construct three datasets denoted as “Historical”, “First” and “Second” respectively.

- Historical: 60% samples from MNIST in χ and used to train the “Historical” model.
- First: the rest 20% samples from MNIST with values in χ and 50% samples from digit zero.
- Second: the rest 20% samples from MNIST with values in χ , the rest 50% samples from digit zero and 50% samples from digit two.

Starting with the fitted “Historical” model using the “Historical” data, we fit AdapVAE only using the “First” dataset. AdapVAE detects the novel cluster digit zero with high accuracy. Starting with the fitted model using the “First” dataset, we fit AdapVAE using the “Second” dataset. Similarly, AdapVAE detects the novel cluster digit two with high accuracy.



(a) The tSNE (Maaten and Hinton, 2008) visualization by transforming the ten dimensional latent representation to a two dimensional space. Different colors indicate the ground-truth cluster corresponding to the fitted cluster using AdapVAE. The number of true clusters is ten and eleven clusters are obtained. The extra “mixture” cluster is composed of samples from all digits. We provide the generated image using the posterior mean parameters learnt from AdapVAE, where the last digit corresponds to the mixture cluster. This figure is best viewed in color.



(b) Generated samples using the online fitted AdapVAE parameters. The last row represents the mixture cluster, where digit seven samples are the major elements in the mixture cluster.

Figure 2: Novelty detection and generated samples.

In Figure 2a, we visualize the clustering results using the “Second” dataset to show AdapVAE can detect novel cluster digit two and zero. A similar figure is provided in Figure 1 in the Supplement to show successful detection of digit zero using the “First” dataset. We summarize the clustering results across five replications in Table S5. The precision and recall results for each cluster are provided in Table 3, 4 and 5 in the Supplement.

Table 3: Clustering quality (%) comparison fitting AdapVAE using constructed “Historical”, “First”, “Second” datasets, respectively. Both the average value and the standard error (in the parenthesis) across five replications are provided.

Dataset	NMI	ARI	HS	VM	ACC
Historical (no 0 and 2)	84.50 (0.750)	82.58 (1.79)	87.02 (0.539)	84.46 (0.770)	92.35 (0.637)
First (with 0 and no 2)	87.20 (1.11)	86.89 (0.76)	88.75 (0.653)	86.78 (0.556)	92.86 (0.564)
Second (with 0 and 2)	86.75 (0.880)	87.19 (1.72)	88.58 (0.731)	86.73 (1.03)	92.88 (0.884)

4.4.1 Clustering Pattern and Generated Images

We show the generated image using the “Second” dataset in Figure 2b. In the fitted model we use to generate the image, AdapVAE starts with one cluster and ends up with eleven clusters, where ten clusters have high purity of the ten digits and the extra one is a mixture cluster, which has samples from all digits that are not written clearly. In different replications, AdapVAE also clusters upright and oblique one or five into two groups and ends up with 12 or 13 clusters.

4.4.2 Clustering Quality Comparison for Different Benchmarks

We first compare the clustering accuracy of AdapVAE with other methods. Other methods fix the number of clusters as the ground truth while AdapVAE starts with one cluster and learns the number of clusters adaptively. AdapVAE can not guarantee to obtain the same number of clusters as the ground-truth. Thus, we extend the ACC definition by allowing m to range over all possible many-to-one mappings between clusters and labels, where multiple small clusters are allowed to be mapped to one ground-truth cluster. In Table 4, similar to Xie et al. (2016) and Jiang et al. (2017), we compare the best clustering performance across various methods. We also run five replications of DEC, VaDE and AdapVAE to compare the averaging clustering quality. The results are summarized in Table 2 of the Supplement. We find that AdapVAE often performs the best.

Table 4: Clustering accuracy (%) comparison on benchmark datasets. The first five lines are taken from Jiang et al. (2017). VAE+DP denotes a two-stage method, which first train an VAE and then feed DPMM with the learned latent representation z . The results of VAE+DP highly depend on the latent representation z . AdapVAE jointly trains and learns the VAE and DPMM simultaneously.

Method	MNIST	REUTERS-10K	STL-10
GMM	53.73	54.72	72.44
AE+GMM	82.18	70.13	79.83
VAE + GMM	72.94	69.56	78.86
DEC	84.3	74.32	80.62
VaDE	94.46	79.83	84.45
VAE+DP	94.45	79.68	56.67
AdapVAE	95.06	80.12	87.23

5 Conclusion

We presented a novel clustering algorithm AdapVAE combining DPMM prior with VAEs. It provides an end-to-end deep representation of the data in a low-dimensional latent space with rich clustering structure. We also provided a joint variational inference algorithm to update both the neural network and DPMM parameters. Our work can determine the number of clusters adaptively and detect novelty in an online fashion. Both qualitative and quantitative analysis for both text and image benchmarks are provided to demonstrate that AdapVAE can capture the deep latent structure in the data while maintaining high clustering quality.

6 Acknowledgements

We would like to acknowledge support for this project from NIH/NHLBI U01HL089856 and NIH/NCI R01CA199673.

References

Ahmed, A. and Xing, E. (2008). Dynamic non-parametric mixture models and the recurrent chinese restaurant process: with applications to evolutionary clustering. In *Proceedings of the 2008 SIAM International Conference on Data Mining*, pages 219–230. SIAM.

Amarbayasgalan, T., Jargalsaikhan, B., and Ryu, K. (2018). Unsupervised novelty detection using deep autoencoders with density based clustering. *Applied Sciences*, 8(9):1468.

Bishop, C. M. (2006). *Pattern recognition and machine learning*. Springer.

Blei, D. M., Jordan, M. I., et al. (2006). Variational inference for dirichlet process mixtures. *Bayesian analysis*, 1(1):121–143.

Coates, A., Ng, A., and Lee, H. (2011). An analysis of single-layer networks in unsupervised feature learning. In *Proceedings of the fourteenth international conference on artificial intelligence and statistics*, pages 215–223.

Deng, J., Dong, W., Socher, R., Li, L.-J., Li, K., and Fei-Fei, L. (2009). Imagenet: A large-scale hierarchical image database. In *2009 IEEE conference on computer vision and pattern recognition*, pages 248–255. Ieee.

Dilokthanakul, N., Mediano, P. A., Garnelo, M., Lee, M. C., Salimbeni, H., Arulkumaran, K., and Shanahan, M. (2016). Deep unsupervised clustering with gaussian mixture variational autoencoders. *arXiv preprint arXiv:1611.02648*.

Goyal, P., Hu, Z., Liang, X., Wang, C., and Xing, E. P. (2017). Nonparametric variational auto-encoders for hierarchical representation learning. In *Proceedings of the IEEE International Conference on Computer Vision*, pages 5094–5102.

He, K., Zhang, X., Ren, S., and Sun, J. (2016). Deep residual learning for image recognition. In *Proceedings of the IEEE conference on computer vision and pattern recognition*, pages 770–778.

Hornik, K. (1991). Approximation capabilities of multilayer feedforward networks. *Neural networks*, 4(2):251–257.

Hubert, L. and Arabie, P. (1985). Comparing partitions. *Journal of classification*, 2(1):193–218.

Hughes, M. C. and Sudderth, E. (2013). Memoized online variational inference for dirichlet process mixture models. In *Advances in Neural Information Processing Systems*, pages 1133–1141.

Ishwaran, H. and James, L. F. (2001). Gibbs sampling methods for stick-breaking priors. *Journal of the American Statistical Association*, 96(453):161–173.

Jiang, Z., Zheng, Y., Tan, H., Tang, B., and Zhou, H. (2017). Variational deep embedding: an unsupervised and generative approach to clustering. In *Proceedings of the 26th International Joint Conference on Artificial Intelligence*, pages 1965–1972. AAAI Press.

Johnson, M., Duvenaud, D. K., Wiltschko, A., Adams, R. P., and Datta, S. R. (2016). Composing graphical models with neural networks for structured representations and fast inference. In *Advances in neural information processing systems*, pages 2946–2954.

Kilinc, O. and Uysal, I. (2018). Learning latent representations in neural networks for clustering through pseudo supervision and graph-based activity regularization. *arXiv preprint arXiv:1802.03063*.

Kingma, D. P. and Ba, J. (2014). Adam: A method for stochastic optimization. *arXiv preprint arXiv:1412.6980*.

Kingma, D. P., Mohamed, S., Rezende, D. J., and Welling, M. (2014). Semi-supervised learning with deep generative models. In *Advances in neural information processing systems*, pages 3581–3589.

Kingma, D. P. and Welling, M. (2014). Auto-encoding variational bayes. In *International Conference on Learning Representations (ICLR)*.

Kodirov, E., Xiang, T., Fu, Z., and Gong, S. (2015). Unsupervised domain adaptation for zero-shot learning. In *The IEEE International Conference on Computer Vision (ICCV)*.

LeCun, Y., Bottou, L., Bengio, Y., Haffner, P., et al. (1998). Gradient-based learning applied to document recognition. *Proceedings of the IEEE*, 86(11):2278–2324.

Lewis, D. D., Yang, Y., Rose, T. G., and Li, F. (2004). Rcv1: A new benchmark collection for text categorization research. *Journal of machine learning research*, 5(Apr):361–397.

Maaten, L. v. d. and Hinton, G. (2008). Visualizing data using t-sne. *Journal of machine learning research*, 9(Nov):2579–2605.

MacQueen, J. et al. (1967). Some methods for classification and analysis of multivariate observations. In *Proceedings of the fifth Berkeley symposium on mathematical statistics and probability*, volume 1, pages 281–297. Oakland, CA, USA.

Masana, M., Ruiz, I., Serrat, J., van de Weijer, J., and Lopez, A. M. (2018). Metric learning for novelty and anomaly detection. *arXiv preprint arXiv:1808.05492*.

Nalisnick, E., Hertel, L., and Smyth, P. (2016). Approximate inference for deep latent gaussian mixtures. In *NIPS Workshop on Bayesian Deep Learning*, volume 2.

Rosenberg, A. and Hirschberg, J. (2007). V-measure: A conditional entropy-based external cluster evaluation measure. In *Proceedings of the 2007 joint conference on empirical methods in natural language processing and computational natural language learning (EMNLP-CoNLL)*.

Sethuraman, J. and Tiwari, R. C. (1982). Convergence of dirichlet measures and the interpretation of their parameter. In *Statistical decision theory and related topics III*, pages 305–315. Elsevier.

Williams, G., Baxter, R., He, H., Hawkins, S., and Gu, L. (2002). A comparative study of rnn for outlier detection in data mining. In *2002 IEEE International Conference on Data Mining, 2002. Proceedings.*, pages 709–712. IEEE.

Xie, J., Girshick, R., and Farhadi, A. (2016). Unsupervised deep embedding for clustering analysis. In *International conference on machine learning*, pages 478–487.

Adaptive Nonparametric Variational Autoencoder Supplement

1 Variational Inference for AdapVAE and ELBO Derivation

In this section, we provide the ELBO derivation. Recall that we use the variational distribution $q(\mathbf{y}, \mathbf{z}, \boldsymbol{\phi}, \mathbf{v}|\mathbf{x})$ to approximate the posterior distribution $p(\mathbf{y}, \mathbf{z}, \boldsymbol{\phi}, \mathbf{v}|\mathbf{x})$. Minimizing the Kullback-Leibler (KL) divergence between $q(\mathbf{y}, \mathbf{z}, \boldsymbol{\phi}, \mathbf{v}|\mathbf{x})$ and $p(\mathbf{y}, \mathbf{z}, \boldsymbol{\phi}, \mathbf{v}|\mathbf{x})$ is equivalent to maximizing the ELBO $\mathcal{L}_{\text{ELBO}}$. We first list the assumptions on the variational distribution $q(\mathbf{y}, \mathbf{z}, \boldsymbol{\phi}, \mathbf{v}|\mathbf{x})$ and then provide the ELBO derivation and the updating equations.

We assume that

$$\begin{aligned} q(\mathbf{y}, \mathbf{z}, \boldsymbol{\phi}, \mathbf{v}|\mathbf{x}) &= q_{\psi}(\mathbf{z}|\mathbf{x})q(\mathbf{y}, \mathbf{z}, \boldsymbol{\phi}|\mathbf{x}) \\ &= q_{\psi}(\mathbf{z}|\mathbf{x})q(\mathbf{y})q(\mathbf{v})q(\boldsymbol{\phi}). \end{aligned}$$

Now, we list the variational distribution assumptions for $q_{\psi}(\mathbf{z}|\mathbf{x})$, $q(\mathbf{y})$, $q(\mathbf{v})$ and $q(\boldsymbol{\phi})$ respectively.

$$q(\mathbf{y}, \mathbf{v}, \boldsymbol{\phi}|\mathbf{x}) = \prod_{t=1}^{T-1} q_{\eta_t}(v_t) \prod_{t=1}^T q_{\zeta_t}(\boldsymbol{\phi}_t) \prod_{n=1}^N q_{\rho_n}(y_n), \quad (4)$$

where T is the number of mixture components in the DP of the variational distribution and $\mathbf{z}_n \sim \mathcal{N}(\mathbf{z}_n|\mu_t, \Lambda_t^{-1})$.

- $q_{\psi}(\mathbf{z}|\mathbf{x}) = \mathcal{N}(\boldsymbol{\mu}(\mathbf{x}; \psi), \boldsymbol{\sigma}^2(\mathbf{x}; \psi))$
- $q_{\zeta_t}(\boldsymbol{\phi}_t) = q(\mu_t|\Lambda_t)q(\Lambda_t) = \mathcal{N}(\mu_t|m_t, (\beta_t \Lambda_t)^{-1})\mathcal{W}(\Lambda_t|W_t, \nu_t)$, where $\boldsymbol{\phi}_t = (\mu_t, \Lambda_t)$.
- $q(y_n) = \text{Mult}(T, \rho_n)$, which is a Multinomial distribution.
- $q_{\eta_t}(v_t) = \text{Beta}(\eta_{t1}, \eta_{t2})$.

Under our assumptions, the $\mathcal{L}_{\text{ELBO}}(\mathbf{x})$ can be rewritten as:

$$\begin{aligned} \mathcal{L}_{\text{ELBO}}(\mathbf{x}) &= \mathbb{E}_{q(\mathbf{y}, \mathbf{z}, \boldsymbol{\phi}, \mathbf{v}|\mathbf{x})} \left[\log \frac{p(\mathbf{x}, \mathbf{y}, \mathbf{z}, \boldsymbol{\phi}, \mathbf{v})}{q(\mathbf{y}, \mathbf{z}, \boldsymbol{\phi}, \mathbf{v}|\mathbf{x})} \right] \\ &= \mathbb{E}_{q(\mathbf{y}, \mathbf{z}, \boldsymbol{\phi}, \mathbf{v}|\mathbf{x})} \left[\log \frac{p(\mathbf{x}|\mathbf{z})p(\mathbf{z}|\mathbf{y}, \boldsymbol{\phi})p(\mathbf{y}|\mathbf{v})p(\mathbf{v})p(\boldsymbol{\phi})}{q_{\psi}(\mathbf{z}|\mathbf{x})q(\mathbf{y}|\mathbf{x})q(\mathbf{v})q(\boldsymbol{\phi}|\mathbf{x})} \right] \\ &= \mathbb{E}_{q(\mathbf{y}, \mathbf{z}, \boldsymbol{\phi}, \mathbf{v}|\mathbf{x})} [\log p(\mathbf{x}|\mathbf{z})] + \mathbb{E}_{q(\mathbf{y}, \mathbf{z}, \boldsymbol{\phi}, \mathbf{v}|\mathbf{x})} [\log p(\mathbf{z}|\mathbf{y}, \boldsymbol{\phi})] \\ &\quad + \mathbb{E}_{q(\mathbf{y}, \mathbf{z}, \boldsymbol{\phi}, \mathbf{v}|\mathbf{x})} [\log p(\mathbf{y}|\mathbf{v})] + \mathbb{E}_{q(\mathbf{y}, \mathbf{z}, \boldsymbol{\phi}, \mathbf{v}|\mathbf{x})} [\log p(\mathbf{v})] \\ &\quad + \mathbb{E}_{q(\mathbf{y}, \mathbf{z}, \boldsymbol{\phi}, \mathbf{v}|\mathbf{x})} [\log p(\boldsymbol{\phi})] - \mathbb{E}_{q(\mathbf{y}, \mathbf{z}, \boldsymbol{\phi}, \mathbf{v}|\mathbf{x})} [\log q_{\psi}(\mathbf{z}|\mathbf{x})] \\ &\quad - \mathbb{E}_{q(\mathbf{y}, \mathbf{z}, \boldsymbol{\phi}, \mathbf{v}|\mathbf{x})} [\log q(\mathbf{y}|\mathbf{x})] - \mathbb{E}_{q(\mathbf{y}, \mathbf{z}, \boldsymbol{\phi}, \mathbf{v}|\mathbf{x})} [\log q(\mathbf{v})] \\ &\quad - \mathbb{E}_{q(\mathbf{y}, \mathbf{z}, \boldsymbol{\phi}, \mathbf{v}|\mathbf{x})} [\log q(\boldsymbol{\phi}|\mathbf{x})] \end{aligned} \quad (5)$$

In our updating strategy, we adopt an alternating optimization strategy used by Goyal et al. (2017). To be specific, we update the VAE parameters (θ and ψ) and the latent variable (\mathbf{z}) given the current estimates of the DPMM parameters. When updating the DPMM parameters, the latent representation \mathbf{z} is treated as the observations for DPMM. The updates for the local cluster membership assignment parameter \mathbf{y} , global parameters $\boldsymbol{\phi}$ and \mathbf{v} simplifies to the updates in variational inference for DPMM developed by Blei et al. (2006). Hence, we only list the updating equations and the expectation derivation involving $q(\mathbf{y})$, $q(\boldsymbol{\phi})$ and $q(\mathbf{v})$ at the end of this section. The notation summary is provided in the main paper. We focus on deriving the nonstandard terms involving the VAE parameters θ , ψ and latent representation \mathbf{z} first.

(1) $\mathbb{E}_{q_\psi(\mathbf{z}|\mathbf{x})q(\mathbf{y})q(\mathbf{v})q(\phi)}[\log P_\theta(\mathbf{x}|\mathbf{z})]$:

We use a neural network g to model the decoder with parameters θ , where $(\boldsymbol{\mu}_{\mathbf{x}}, \log \boldsymbol{\sigma}_{\mathbf{x}}^2) = g_\theta(\mathbf{z})$ and $P_\theta(\mathbf{x}|\mathbf{z}) = \mathcal{N}(\mathbf{x}; \boldsymbol{\mu}_{\mathbf{x}}, \boldsymbol{\sigma}_{\mathbf{x}}^2 \mathbf{I})$. Hence, we have

$$\begin{aligned} \mathbb{E}_{q_\psi(\mathbf{z}|\mathbf{x})q(\mathbf{y})q(\mathbf{v})q(\phi)}[\log P_\theta(\mathbf{x}|\mathbf{z})] &= \mathbb{E}_{q_\psi(\mathbf{z}|\mathbf{x})q(\mathbf{y})q(\mathbf{v})q(\phi)} \left(-\frac{1}{2} \log(\boldsymbol{\sigma}_{\mathbf{x}}^2)_j + \frac{(\mathbf{x}_j - (\boldsymbol{\mu}_{\mathbf{x}})_j)^2}{(\boldsymbol{\sigma}_{\mathbf{x}}^2)_j} \right) \\ &= -\frac{1}{2} \frac{1}{L} \sum_{i=1}^N \sum_{j=1}^D \left(\log(\boldsymbol{\sigma}_{\mathbf{x}}^2)_j^{(l)} + \frac{(\mathbf{x}_{ij} - (\boldsymbol{\mu}_{\mathbf{x}})_j^{(l)})^2}{(\boldsymbol{\sigma}_{\mathbf{x}}^2)_j^{(l)}} \right), \end{aligned} \quad (6)$$

where

- $(\boldsymbol{\mu}_{\mathbf{x}})_j$: represents the j th element of $\boldsymbol{\mu}_{\mathbf{x}}$ for $j = 1, 2, \dots, D$.
- $(\boldsymbol{\sigma}_{\mathbf{x}}^2)_j$: represents the j th element of $\boldsymbol{\sigma}_{\mathbf{x}}^2$ for $j = 1, 2, \dots, D$.
- \mathbf{x}_{ij} : represents the j th element of the i th observation.

(2) $\mathbb{E}_{q_\psi(\mathbf{z}|\mathbf{x})q(\mathbf{y})q(\mathbf{v})q(\phi)}[\log p(\mathbf{z}|\mathbf{y}, \phi)]$:

We use neural network f to model the encoder with parameters ψ , where $q_\psi(\mathbf{z}|\mathbf{x}) = \mathcal{N}(\boldsymbol{\mu}(\mathbf{x}; \psi), \boldsymbol{\sigma}^2(\mathbf{x}; \psi))$ and $(\boldsymbol{\mu}(\mathbf{x}; \psi), \log \boldsymbol{\sigma}^2(\mathbf{x}; \psi)) = f(\mathbf{x}; \psi)$. In VAE, we use the reparameterization trick to allow backpropagation:

$$\boldsymbol{\epsilon}^{(l)} \sim \mathcal{N}(\mathbf{0}, \mathbf{I}) \text{ and } \mathbf{z}^{(l)} = \boldsymbol{\mu}(\mathbf{x}; \psi) + \boldsymbol{\epsilon}^{(l)} \boldsymbol{\sigma}(\mathbf{x}; \psi).$$

We denote $\hat{\mathbf{z}}_n$ as the estimated mean of the latent representation from the encoder given \mathbf{x}_n :

$$\hat{\mathbf{z}}_n = g_\mu(\mathbf{x}_n; \phi) = \boldsymbol{\mu}(\mathbf{x}_n; \psi) = \lim_{L \rightarrow \infty} \frac{1}{L} \sum_{l=1}^L \mathbf{z}_n^{(l)}.$$

According to Equation 10.71 of Bishop (2006), we have the following:

$$\begin{aligned} &\mathbb{E}_{q_\psi(\mathbf{z}|\mathbf{x})q(\mathbf{y})q(\mathbf{v})q(\phi)}[\log p(\mathbf{z}|\mathbf{y}, \phi)] \\ &= \frac{1}{2} \sum_{k=1}^T N_k \left\{ \log \tilde{\Lambda}_k - D \beta_k^{-1} - \nu_k \text{Tr}(S_k W_k) - \nu_k (\bar{\mathbf{z}}_k - \mathbf{m}_k)^T W_k (\bar{\mathbf{z}}_k - \mathbf{m}_k) - D \log(2\pi) \right\}, \end{aligned} \quad (7)$$

where

$$\begin{aligned} \mathbb{E}_{\phi_k} \left[(\hat{\mathbf{z}}_n - \boldsymbol{\mu}_k)^T \Lambda_k (\hat{\mathbf{z}}_n - \boldsymbol{\mu}_k) \right] &= \frac{D}{\beta_k} + \nu_k (\hat{\mathbf{z}}_n - \mathbf{m}_k)^T W_k (\hat{\mathbf{z}}_n - \mathbf{m}_k) \\ \log \tilde{\Lambda}_k &= \mathbb{E}[\log \Lambda_k] = \sum_{j=1}^D \psi \left(\frac{\nu_k + 1 - j}{2} \right) + D \log 2 + \log |W_k|. \end{aligned} \quad (8)$$

(3) $\mathbb{E}_{q_\psi(\mathbf{z}|\mathbf{x})q(\mathbf{y})q(\mathbf{v})q(\phi)}(\log q_\psi(\mathbf{z}|\mathbf{x}))$:

We assume that $q_\psi(\mathbf{z}|\mathbf{x}) = \mathcal{N}(\boldsymbol{\mu}(\mathbf{x}; \psi), \boldsymbol{\sigma}^2(\mathbf{x}; \psi))$. Hence, $\mathbb{E}_{q_\psi(\mathbf{z}|\mathbf{x})q(\mathbf{y})q(\mathbf{v})q(\phi)}(\log q_\psi(\mathbf{z}|\mathbf{x}))$ is equal to the negative entropy of a multivariate Gaussian distribution, which is:

$$\mathbb{E}_{q_\psi(\mathbf{z}|\mathbf{x})q(\mathbf{y})q(\mathbf{v})q(\phi)}(\log q_\psi(\mathbf{z}|\mathbf{x})) = \frac{1}{2} \log(\text{Det}(2\pi e \Sigma)) \quad (9)$$

where $\Sigma = \boldsymbol{\sigma}^2(\mathbf{x}; \psi) \mathbf{I}$.

When we update the VAE parameters θ and ψ and the latent representation \mathbf{z} , the DPMM parameters will be fixed. Thus, the terms that do not involve \mathbf{z} , θ , ψ will not contribute to the L_{ELBO} . Hence, by combining Equation 6, 7 and 9, we obtain

$$\begin{aligned}\mathcal{L}_{\text{ELBO}}(\mathbf{x}) = & -\frac{1}{2L} \sum_{l=1}^L \sum_{k=1}^T N_k \nu_k \left\{ \text{Tr}(S_k W_k) + (\bar{z}_k - \mathbf{m}_k)^T W_k (\bar{z}_k - \mathbf{m}_k) \right\} \\ & - \frac{1}{2} \frac{1}{L} \sum_{i=1}^N \sum_{j=1}^D \left(\log(\sigma_x^2)_j^{(l)} + \left(\mathbf{x}_{ij} - (\mu_x)_j^{(l)} \right)^2 / (\sigma_x^2)_j^{(l)} \right) + \frac{1}{2} \log(\text{Det}(2\pi e \Sigma)). \quad (10)\end{aligned}$$

Here, we list the standard variational inference updating equations and derivations for DPMM.

- $q(\mathbf{y}_n = i) = \gamma_{n,i}$.
- $q(\mathbf{y}_n > i) = \sum_{j=i+1}^T \gamma_{n,j}$.
- $\mathbb{E}_q[\log V_i] = \Psi(\gamma_{i,1}) - \Psi(\gamma_{i,1} + \gamma_{i,2})$.
- $\mathbb{E}_q[\log(1 - V_i)] = \Psi(\gamma_{i,2}) - \Psi(\gamma_{i,1} + \gamma_{i,2})$.
- $\gamma_{n,t} \propto \exp(S_t)$,
- $S_t = \mathbb{E}[\log V_i] + \sum_{i=1}^{t-1} \mathbb{E}_q[\log(1 - V_i)] + \frac{1}{2} \log \tilde{\Lambda}_k - \frac{D}{2\beta_k} - \frac{\nu_k}{2} (\hat{z}_n - \mathbf{m}_k)^T W_k (\hat{z}_n - \mathbf{m}_k)$.
- $\gamma_{n,t} = \frac{\exp(S_t)}{\sum_{t=1}^T \exp(S_t)}$.
- Under the Gaussian-Wishart distribution assumption,

$$\begin{aligned}\mathbb{E} q_\psi(\mathbf{z}|\mathbf{x}) q(\mathbf{y}) q(\mathbf{v}) q(\boldsymbol{\phi}) (\log p(\boldsymbol{\phi})) \\ = \frac{1}{2} \sum_{k=1}^T \left\{ D \log(\beta_0/2\pi) + \log \tilde{\Lambda}_k - \frac{D\beta_0}{\beta_k} - \beta_0 \nu_k (\mathbf{m}_k - \mathbf{m}_0)^T W_k (\mathbf{m}_k - \mathbf{m}_0) \right\} \\ + T \log B(W_0, \nu_0) \frac{\nu_0 - D - 1}{2} \sum_{k=1}^T \log \tilde{\Lambda}_k - \frac{1}{2} \sum_{i=1}^T \nu_k \text{Tr}(W_0^{-1} W_k),\end{aligned}$$

where

$$B(W, \nu) = |W|^{-\nu/2} \left(2^{\nu D/2} \pi^{D(D-1)/4} \prod_{i=1}^D \Gamma \left(\frac{\nu + 1 - i}{2} \right) \right)^{-1}.$$

- Similarly, we have

$$\mathbb{E} q_\psi(\mathbf{z}|\mathbf{x}) q(\mathbf{y}) q(\mathbf{v}) q(\boldsymbol{\phi}) [\log q(\boldsymbol{\phi})] = \sum_{k=1}^T \left(\frac{1}{2} \log \tilde{\Lambda}_k + \frac{D}{2} \log \left(\frac{\beta_k}{2\pi} \right) - \frac{D}{2} - H[q(\Lambda_k)] \right)$$

where

$$H[\Lambda] = -\log B(W, \nu) - \frac{\nu - D - 1}{2} \mathbb{E}[\log \Lambda] + \frac{\nu D}{2}.$$

A summary of notations for deriving the ELBO is listed below.

2 Benchmark Datasets Description

- **MNIST**: The MNIST dataset consists images of 70000 handwritten digits of 28×28 pixel size. In order to compare fairly with previous methods, we did normalization and flattened each image to a 784×1 vector.
- **STL-10**: The STL-10 dataset consists of color images of 96×96 pixel size. There are 10 classes with 1300 examples each. Following previous works, we fed original images to ResNet (He et al. (2016)) pretrained on ImageNet (Deng et al. (2009)) and used the last feature map after the 3×3 average pooling layer. So the extracted feature is of size 2048×1 .

Table S1: Notations in the ELBO.

Notations in the ELBO
N : the total number of observations.
L : the number of samples we obtain when using SGVB and representation trick for VAE.
Σ : the diagonal covariance matrix of the encoder.
\mathbf{x}_n : the n th observation.
$p(\mathbf{y}_i = k) = \gamma_{ik}$: the probability of the i th observation in the k th cluster.
$N_k = \sum_{n=1}^N \gamma_{nk}$: the sum of the probability of the total N observations in the k th cluster.
$\hat{\mathbf{z}}_n = \boldsymbol{\mu}(\mathbf{x}_n; \psi)$: the estimated mean of the latent representation from the encoder given \mathbf{x}_n .
$\bar{\mathbf{z}}_k = \frac{1}{N_k} \sum_{n=1}^N \gamma_{nk} \hat{\mathbf{z}}_n$: the weighted mean of the k th cluster in the latent representation space.
$S_k = \frac{1}{N_k} \sum_{n=1}^N \gamma_{nk} (\hat{\mathbf{z}}_n - \bar{\mathbf{z}}_k)(\hat{\mathbf{z}}_n - \bar{\mathbf{z}}_k)^T$.
$\beta_k = \beta_0 + N_k$: the scalar precision for \mathbf{z}_k in the Normal-Wishart distribution.
$\mathbf{m}_k = \frac{1}{\beta_k} (\beta_0 \mathbf{m}_0 + N_k \bar{\mathbf{z}}_k)$: the updated formula for the mean of the Normal-Wishart distribution for the k th cluster, where the prior \mathbf{m}_0 is usually chosen as a zero vector.
$W_k^{-1} = W_0^{-1} + N_k S_k + \frac{\beta_0 N_k}{\beta_0 + N_k} (\bar{\mathbf{z}}_k - \mathbf{m}_0)(\bar{\mathbf{z}}_k - \mathbf{m}_0)^T$: the updated formula for W_k^{-1} , the parameter of Normal-Wishart distribution.
$\nu_k = \nu_0 + N_k$: updated degrees of freedom of the Normal-Wishart distribution for the k th cluster.
ϕ : the variational parameters of the Normal Wishart mixing components in the DP.
η_t : the variational parameters of a Beta distribution for the t th component defined in Equation 4.
ζ_t : the variational parameters of the Normal-Wishart distribution for ϕ_t defined in Equation 4.
ρ_n : the variational parameters of the categorical distribution for the cluster membership for each observation.

- **REUTERS**: The Reuters dataset contains about 810000 English news stories labeled with a category tree. Following previous works, we just used four root categories corporate/industrial, government/social, markets, and economics as labels and discard articles have multiple labels to get 685071 articles. We then randomly sampled a subset of 10000 articles called call REUTERS-10K. As our method are scalable by its online nature, we mainly experimented on REUTERS-10K.

3 Evaluation metrics

- **Normalized Mutual Information (NMI)** is a normalized metric for determining the quality of clustering. It can be used to compare different clusterings with different number of clusters. Its range is between zero and one, which represents no mutual information and perfect correlation. The NMI is defined as follows:

$$\text{NMI}(l, c) = \frac{2 * I(l, c)}{[H(l) + H(c)]},$$

where l is the ground-truth label, c is the cluster assignment by the algorithm, I and H represents mutual information and entropy respectively (the definition for I and H is the same among all the following metrics).

- **Adjusted Random Index (ARI)** ranges between zero and one. If it is close to zero, it represents random labeling independently of the number of clusters and samples; it equals to one when the clusterings are identical as the true one (up to a permutation).

Given a set S of n samples, where C is the set of true classes, $C = \{c_i | i = 1, \dots, n_c\}$ and K is the set of clusters, $K = \{k_i | i = 1, \dots, n_k\}$. Define A to be the contingency table produced by the clustering algorithm such that every element a_{ij} in A represents the number of samples that are members of class c_i and elements of cluster k_j . Therefore, the ARI is defined as follows according to Hubert and Arabie (1985):

$$\text{ARI} = \frac{\sum_{ij} \binom{a_{ij}}{2} - [\sum_i \binom{a_i}{2} \sum_j \binom{b_j}{2}] / \binom{n}{2}}{\frac{1}{2} [\sum_i \binom{a_i}{2} + \sum_j \binom{b_j}{2}] - [\sum_i \binom{a_i}{2} \sum_j \binom{b_j}{2}] / \binom{n}{2}},$$

where $a_i = \sum_j a_{ij}$ and $b_j = \sum_i a_{ij}$.

- **Homogeneity Score (HS)** is a homogeneity metric of a cluster labeling given the ground truth. A clustering satisfies homogeneity (with value one) if all of its clusters contain only data points which are members of a single class.

In Rosenberg and Hirschberg (2007), they assume n is number of observations and share the same definition of C , K and A as in ARI. They define homogeneity as:

$$h = \begin{cases} 1 & \text{if } H(C, K) = 0, \\ 1 - \frac{H(C|K)}{H(C)} & \text{else,} \end{cases}$$

$$H(C|K) = - \sum_{k=1}^{|K|} \sum_{c=1}^{|C|} \frac{a_{ck}}{N} \log \frac{a_{ck}}{\sum_{c=1}^{|C|} a_{ck}}$$

$$H(C) = - \sum_{c=1}^{|C|} \frac{\sum_{k=1}^{|K|} a_{ck}}{n} \log \frac{\sum_{k=1}^{|K|} a_{ck}}{n}$$

Since $H(C|K) \leq H(C)$, the value of h is between zero and one. In the degenerate case where $H(C) = 0$, they define h to be 1.

- **V-measure score (VM)** is a metric to measure the agreement of two independent clusterings on the same dataset. Its range is between zero and one where one stands for perfect complete clustering as the ground truth. V-measure is the weighted harmonic mean of homogeneity and completeness. Rosenberg and Hirschberg (2007) define the completeness measure as follows, which is symmetrical to homogeneity defined as HS previously (definitions of parameters are the same as in HS):

$$c = \begin{cases} 1 & \text{if } H(K, C) = 0, \\ 1 - \frac{H(K|C)}{H(K)} & \text{else,} \end{cases}$$

where

$$H(K|C) = - \sum_{c=1}^{|C|} \sum_{k=1}^{|K|} \frac{a_{ck}}{N} \log \frac{a_{ck}}{\sum_{k=1}^{|K|} a_{ck}}$$

$$H(K) = - \sum_{k=1}^{|K|} \frac{\sum_{c=1}^{|C|} a_{ck}}{n} \log \frac{\sum_{c=1}^{|C|} a_{ck}}{n}$$

Similarly, in the degenerate case where $H(K) = 0$, they define c to be 1. The V-measure is defined as follows:

$$V_\beta = \frac{(1 + \beta) * h * c}{(\beta * h) + c}.$$

Where β is the weighting factor. Note that if β is greater than one, completeness is weighted more strongly; if β is less than one, homogeneity is weighted more strongly.

4 Figures

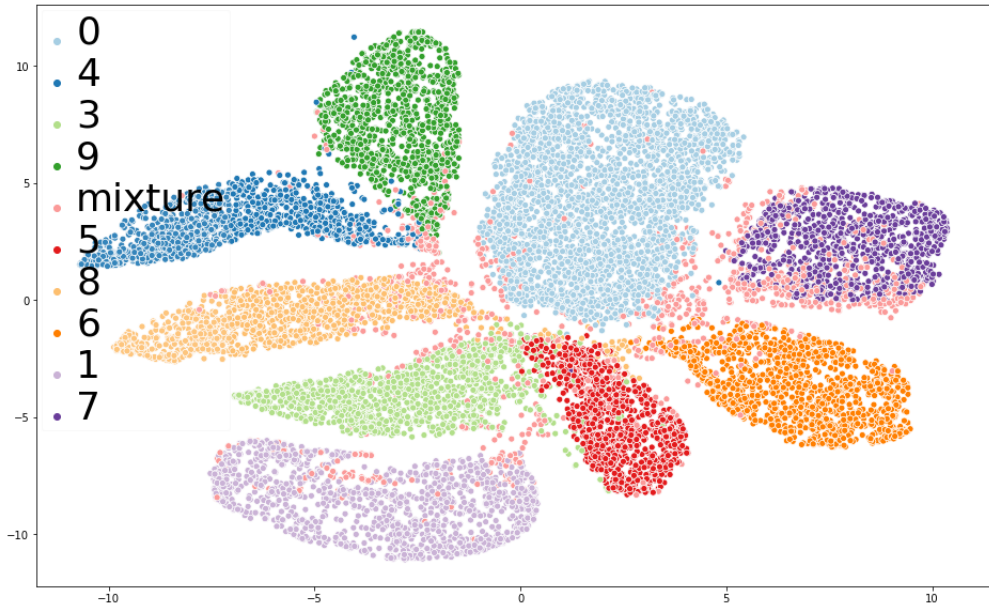


Figure S1: We provide the tSNE (Maaten and Hinton, 2008) plot by transforming the ten dimensional latent representation to a two dimensional space for visualization. Different colors indicate the ground-truth classes corresponding to the fitted classes from our algorithm. The number of true clusters is nine (since the dataset does not include number two) and we obtain ten fitted clusters where the “mixture” cluster is composed of samples from multiple classes. This figure is best viewed in color.

5 Tables

Table S2: Clustering quality (%) comparison on benchmark datasets averaged over five replications. Both the average value and the standard error (in the parenthesis) are provided.

Dataset	Method	NMI	ARI	HS	VM	ACC
MNIST	DEC	84.67 (2.25)	83.67 (4.53)	84.67 (2.25)	84.67 (2.25)	91.04 (3.39)
	VaDE	80.35 (4.68)	74.06 (9.11)	79.86 (4.93)	80.36 (4.69)	80.87 (9.15)
	VAE+DP	81.70 (0.825)	70.49 (1.654)	91.27 (0.215)	81.19 (0.904)	94.23 (0.183)
	AdapVAE	85.72 (1.02)	83.53 (2.35)	89.34 (0.25)	85.65 (0.51)	93.85 (0.51)
Reuters10k	DEC	46.56 (5.36)	46.86 (7.98)	48.44 (5.44)	46.52 (5.36)	67.27 (4.56)
	VaDE	41.64 (4.73)	38.49 (5.44)	43.64 (4.88)	41.60 (4.73)	63.8 (5.08)
	VAE + DP	41.62 (2.99)	37.93 (4.57)	46.64 (3.85)	41.34 (2.94)	78.14 (2.25)
	AdapVAE	45.32 (1.79)	42.66 (5.73)	48.88 (1.86)	45.40 (2.04)	78.32 (1.79)
STL10	DEC	71.92 (2.66)	58.73 (5.09)	68.47 (3.48)	71.83 (2.72)	66.89 (4.26)
	VaDE	68.35 (3.85)	59.42 (6.84)	67.24 (4.23)	68.37 (3.92)	72.10 (7.40)
	VAE+DP	43.18 (1.41)	26.58 (1.32)	42.28 (1.03)	43.16 (1.39)	55.21 (1.45)
	AdapVAE	75.26 (0.53)	70.72 (0.81)	77.61 (1.29)	75.22 (0.52)	85.28 (1.40)

Table S3: Precision and recall for each cluster using the "Historical" data without zero or two on MNIST. Number seven has the major contribution to the mixture cluster.

Precision	Recall	TrueClass	FittedClass
0.999	0.914	1	1
0.908	0.962	3	0
0.952	0.97	4	3
0.996	0.837	5	7
0.997	0.901	6	5
0.995	0.78	7	6
0.909	0.935	8	3
0.992	0.885	9	4
0.4	0.214	Mixture (7)	8

Table S4: Precision and recall for each cluster using the "First" dataset with number zero as the novel class on MNIST. Number seven has the major contribution to the mixture cluster.

Precision	Recall	TrueClass	FittedClass
0.999	0.937	0	0
0.9986	0.9127	1	2
0.9095	0.9473	3	1
0.972	0.975	4	3
0.973	0.923	5	8
0.995	0.932	6	5
0.994	0.741	7	7
0.973	0.923	8	6
0.996	0.921	9	4
0.333	0.254	Mixture (7)	9

Table S5: Precision and recall for each cluster using the "Second" dataset with number two as the novel class on MNIST. Number seven has the major contribution to the mixture class.

Precision	Recall	TrueClass	FittedClass
0.998	0.96	0	1
1.000	0.904	1	5
0.976	0.967	2	0
0.918	0.91	3	4
0.987	0.964	4	8
0.991	0.834	5	7
0.995	0.937	6	2
0.992	0.712	7	10
0.942	0.948	8	3
0.989	0.939	9	6
0.366	0.283	Mixture (7)	9